

Reactions of Fe⁺, Co⁺, and Ni⁺ with Silane. Electronic State Effects, Comparison to Reactions with Methane, and M⁺–SiH_x (x = 0–3) Bond Energies

Bernice L. Kickel and P. B. Armentrout*

Contribution from the Department of Chemistry, University of Utah, Salt Lake City, Utah 84112

Received June 20, 1994[Ⓢ]

Abstract: Guided ion beam techniques are used to measure cross sections as a function of kinetic energy for the reaction of SiH₄ with M⁺ = Fe⁺, Co⁺, and Ni⁺. Ionic products include MSiH_x⁺ (x = 0–3), as well as MH⁺ and SiH₃⁺. No structural information concerning the MSiH_x⁺ species is obtained in the present results. The major low-energy process in all three systems is formation of MSiH₂⁺ + H₂, while at higher energies, formation of MH⁺ + SiH₃ (M = Fe and Co) or SiH₃⁺ + MH (M = Ni) dominates the reactivity. Variation of source conditions allows the effect of electronic excitation on the reactivity of Fe⁺ to be studied in detail. The a⁴F first excited state of Fe⁺ is more reactive by approximately an order of magnitude than the a⁶D ground state and has a different product distribution. The reactivity of Fe⁺ (a⁴F) is found to closely resemble that of ground state Co⁺ (a³F), which is approximately half as reactive as ground state Ni⁺ (a²D). The reactivity of these systems may be understood in terms of simple molecular orbital and spin conservation arguments. The thresholds for Fe⁺, Co⁺, and Ni⁺ reactions are evaluated to yield 0 K bond dissociation energies (BDEs) for M⁺–Si, M⁺–SiH, M⁺–SiH₂, and M⁺–SiH₃ of 2.87 ± 0.09, 2.63 ± 0.13, 1.88 ± 0.09, and 1.90 ± 0.09 eV, respectively, for M = Fe; 3.25 ± 0.07, 3.03 ± 0.16, 2.25 ± 0.08, and 1.96 ± 0.13 eV, respectively, for M = Co; and 3.34 ± 0.07, 3.38 ± 0.15, ≥2.39 ± 0.07, and 1.91 ± 0.12 eV, respectively, for M = Ni. Evaluation of thresholds for SiH₃⁺ + MH formation (M = Fe, Co, and Ni) is combined with previous studies in our laboratories to yield 0 K BDEs for Fe–H of 1.52 ± 0.05 eV, for Co–H of 1.95 ± 0.05 eV, and for Ni–H of 2.56 ± 0.11 eV.

Introduction

A number of reactions, such as hydrosilation,^{1,2} silane polymerization,³ and chemical vapor deposition of transition metal silicides,⁴ are thought to proceed through transition metal–silicon complexes. In an effort to provide a more fundamental understanding of such species, we recently initiated a series of experiments on the gas-phase reactivity of atomic transition metal ions with silane.⁵ The present work concentrates on the reactions of silane with Fe⁺, Co⁺, and Ni⁺. Previous work of relevance to these systems includes studies by Kang *et al.*,⁶ who investigated the reactions of silane and organosilanes with Fe⁺, Co⁺, and Ni⁺. Bakhtiar *et al.*⁷ provided the first examples of the generation of stable isomeric Fe⁺–silene and Fe⁺–silylene complexes in the gas phase. Theoretical studies include those by Cundari and Gordon⁸ on first-row transition metal silylenes (MSiH₂⁺) where M = Sc–Ni, those by Musaev *et al.*⁹ on comparisons of MCH₂⁺ and MSiH₂⁺ (M = Co, Rh, and Ir) complexes, and those by Ferhati and Ohanessian on the potential energy surfaces of the analogous reaction of silane with Y⁺.¹⁰

In the present study, the kinetic energy dependence of the reactions of Fe⁺, Co⁺, and Ni⁺ with silane is studied in detail by using guided ion beam mass spectrometry. The kinetic energy dependence of the cross sections is analyzed to yield M⁺–SiH_x (x = 0–3) bond energies. In addition, variation of the ion source conditions allows us to explicitly evaluate contributions of two electronic states of Fe⁺ to the observed reactivity. This work is based on previous state-specific studies of Fe⁺ with dihydrogen¹¹ and methane, ethane, and propane.¹² Thermodynamic and state-specific results are combined to provide information regarding likely reaction mechanisms. Comparison of transition metal–silicon versus transition metal–carbon bond energies aids our understanding of the trends in metal–silicon thermochemistry.

Experimental Section

General. Complete descriptions of the apparatus and experimental procedures are given elsewhere.^{13,14} Briefly, ions are produced as described below, accelerated, and focused into a magnetic sector momentum analyzer for mass analysis. They are then decelerated to the desired translational energy and focused into an octopole ion beam guide¹⁵ that traps ions in the radial direction. The octopole passes through a static gas cell into which the neutral gas is introduced at sufficiently low pressures, 0.05–0.15 mTorr, that multiple ion–molecule collisions are improbable. Pressure-dependent studies verify that the cross sections measured here are due to single ion–molecule

[Ⓢ] Abstract published in *Advance ACS Abstracts*, January 1, 1995.

(1) Noll, W. *Chemistry and Technology of Silicons*; Academic: New York, 1986.

(2) Stone, F. G. A.; West, R., Eds. *Advances in Organometallic Chemistry*; Academic: San Diego, CA, 1990.

(3) For a review of polysilane polymers, see: West, R. *J. Organomet. Chem.* **1986**, *300*, 327.

(4) Corey, J. Y.; Corey, E. R.; Gaspar, P. P., Eds. *Silicon Chemistry*; Harwood: Chichester, England, 1988; Chapters 30, 32, and 33.

(5) Kickel, B. L.; Armentrout, P. B. *J. Am. Chem. Soc.* **1994**, *116*, 10742.

(6) Kang, H.; Jacobson, D. B.; Shin, S. K.; Beauchamp, J. L.; Bowers, M. T. *J. Am. Chem. Soc.* **1986**, *108*, 5668.

(7) Bakhtiar, R.; Holznagel, C.; Jacobson, D. B. *J. Am. Chem. Soc.* **1993**, *115*, 345.

(8) Cundari, T. R.; Gordon, M. S. *J. Phys. Chem.* **1992**, *96*, 631.

(9) Musaev, D. G.; Morokuma, K.; Koga, N. *J. Chem. Phys.* **1993**, *99*, 7859.

(10) Ferhati, A. Ph.D. Thesis, Universite de Paris-Sud, 1994. Ohanessian, G. Personal communication, 1994.

(11) Elkind, J. L.; Armentrout, P. B. *J. Am. Chem. Soc.* **1986**, *108*, 2765; *J. Phys. Chem.* **1986**, *90*, 5736.

(12) Schultz, R. H.; Elkind, J. L.; Armentrout, P. B. *J. Am. Chem. Soc.* **1988**, *110*, 411.

(13) Ervin, K. M.; Armentrout, P. B. *J. Chem. Phys.* **1985**, *83*, 166.

(14) Schultz, R. H.; Armentrout, P. B. *Int. J. Mass Spectrom. Ion Processes* **1991**, *107*, 29.

(15) Teloy, E.; Gerlich, D. *Chem. Phys.* **1974**, *4*, 417.

interactions. After leaving the octopole, transmitted reactant and product ions are extracted and analyzed in a quadrupole mass filter. Ions are detected by a secondary electron scintillation ion counter and processed with pulse counting techniques. Raw ion intensities are converted to absolute reaction cross sections as described previously with uncertainties estimated as $\pm 20\%$.¹³

Laboratory ion energies (lab) are converted to energies in the center-of-mass frame (CM) by using $E_{CM} = E_{lab}M/(m + M)$, where m is the mass of the ion and M is the mass of the silane reactant. The absolute energy and energy distribution of the ions in the interaction region are measured by using the octopole as a retarding field analyzer.¹³ These measurements show that the distribution of ion energies is Gaussian with typical full widths at half-maximum (fwhm) of ~ 0.6 (lab). The uncertainty in the absolute energy scale is ± 0.05 eV (lab). The thermal motion of the gas in the reaction cell has a distribution with a fwhm of $\sim 0.4E_{CM}^{1/2}$ eV.¹⁶ At very low energies, the slower ions in the kinetic energy distribution of the beam are not transmitted through the octopole, resulting in a narrowing of the ion energy distribution. We take advantage of this effect to access very low interaction energies as described previously.^{13,17}

Ion Source. A dc-discharge flow tube (DC/FT) ion source, described in detail previously,¹⁴ is used to form Fe⁺, Co⁺, and Ni⁺ ions. The dc-discharge is used to ionize and accelerate argon ions into an iron, cobalt, or nickel metal cathode to sputter off the desired atomic metal ion. The resulting ions are swept downstream in a flow of helium and argon at a total pressure of 0.4–0.7 Torr and encounter $>10^5$ collisions with the bath gases. It is believed that most excited electronic states of Fe⁺, Co⁺, and Ni⁺ ions are quenched to their ground state by these collisions. More complete quenching of excited electronic states is accomplished by addition of small amounts of oxygen (5–7 mTorr for Fe⁺) or methane (1–3 mTorr for Co⁺) to the flow.^{18,19} In the case of Ni⁺, altering the percentage (10–13%) of argon in the flow resulted in no systematic changes in the data for the present system. The electronic state population of Fe⁺ generated in the DC/FT source has been characterized previously by examining the reaction of Fe⁺ with water,¹⁸ where we found that less than 2% of the reactant ion beam consisted of the a⁴F first excited state, a distribution characterized approximately by a temperature of 725 ± 100 K. This distribution was verified by running this diagnostic reaction during the present work; however, in the silane results, we find indications of a small amount of higher lying excited states that were not completely quenched by the O₂ addition. These states could account for as little as 0.02% of the beam and are easily accounted for in the cross sections measured here. The quenching efficiency for excited Co⁺ has been verified previously in the reaction of Co⁺ with cyclopropane, where we found that the distribution of electronic states of Co⁺ could be characterized by a Maxwell–Boltzmann distribution at 800 ± 100 K.¹⁹

Ion beams of Fe⁺, Co⁺, and Ni⁺ were also produced in a surface ionization (SI) source. Here, the metal is introduced to the gas phase by vaporizing NiCl₂·6H₂O or CoCl₂·6H₂O in an oven or by passing Fe(CO)₅ through a water-cooled inlet line. The metal-containing vapor is passed over a resistively heated rhenium filament at a temperature of 2200 or 2300 \pm 100 K, as measured by optical pyrometry. Dissociation of the metal halides or iron carbonyl and ionization of the resultant metal atoms occur on the filament. We assume that a Maxwell–Boltzmann distribution accurately describes the populations of the electronic states of Fe⁺, Co⁺, and Ni⁺. The validity of this assumption has been discussed previously,²⁰ and recent work by van Koppen *et al.* has verified this assumption in the case of Co⁺.²¹ For Ni⁺, comparison of the present results for ions generated in the DC/FT and SI sources permitted us to characterize the effective temperature of the Ni⁺ (DC/FT) ions by using a procedure analogous to one outlined previously for Co⁺.¹⁹ The result suggests that the populations of the electronic states of Ni⁺ generated in the DC/FT source can be

Table 1. Electronic States of Fe⁺, Co⁺, and Ni⁺

	state	electron confign	energy, ^a eV	% population	
				DC/FT ^b	SI ^c
Fe ⁺	a ⁶ D	4s3d ⁶	0.052	98.0	78.3
	a ⁴ F	3d ⁷	0.300	2.0	21.3
	a ⁴ D	4s3d ⁶	1.032		0.4
	a ⁴ P	3d ⁷	1.688		<0.1
Co ⁺	a ³ F	3d ⁸	0.086	99.7	85.1
	a ² F	4s3d ⁷	0.515	0.3	14.8
	a ³ P	4s3d ⁷	1.298		0.2
	a ³ P	3d ⁸	1.655		$\ll 0.1$
Ni ⁺	a ² D	3d ⁹	0.075	100	98.8
	a ⁴ F	3d ⁸ 4s	1.160		1.2
	a ² F	3d ⁸ 4s	1.757		0.03

^a Energies are a statistical average over J levels taken from ref 30. ^b Maxwell–Boltzmann distributions at 725, 800, and 1300 K for Fe⁺, Co⁺, and Ni⁺, respectively. Populations are estimated from the diagnostic reactions of Fe⁺ with D₂O,¹⁸ Co⁺ with cyclopropane,¹⁹ and Ni⁺ with SiH₄ (see text). ^c Maxwell–Boltzmann distribution at 2300 K for Fe⁺ and Ni⁺ and 2200 K for Co⁺.

characterized by a Maxwell–Boltzmann distribution at 1300 ± 200 K. The populations of the electronic states of the ions generated in both sources are listed in Table 1.

Thermochemical Analysis. The threshold regions of the experimental reaction cross sections are analyzed by using the empirical model of eq 1. Here, E is the relative kinetic energy, E_0 is the reaction

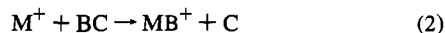
$$\sigma(E) = \sigma_0 \sum_i g_i (E + E_{rot} + E_i - E_0)^n / E \quad (1)$$

endothermicity for reaction of the lowest J state of the ion at 0 K, σ_0 is an energy-independent scaling factor, and n is an adjustable parameter. This equation takes the internal energy of the SiH₄ reagent into consideration by including the average rotational energy, $E_{rot}(\text{SiH}_4) = 3kT/2 = 0.039$ eV at 300 K. Vibrational energy contributions are negligible (<0.007 eV). The summation is over the distribution of electronic states i of the metal ion reactant having energies E_i (Table 1 gives J -averaged values) and relative populations g_i , where $\sum_i g_i = 1$. The resulting model cross section is then convoluted with the ion and neutral translational energy distributions¹³ before comparison with the data. The parameters n , σ_0 , and E_0 are allowed to vary freely to best fit the data as determined by a nonlinear least squares analysis. For analyses of some small cross sections, it was necessary to fix the value of n over an acceptable range while allowing σ_0 and E_0 to vary freely. It is possible that this could introduce systematic errors in the thresholds determined, but the range of n values chosen in each case is large enough to include all likely possibilities. Errors in threshold values, determined by the variation in E_0 among several data sets for all acceptable models and the absolute uncertainty in the energy scale, are believed to be reasonable measures of the absolute accuracy of these threshold values. The general form of eq 1 has been derived as a model for translationally driven reactions²² and has been found to be quite useful in describing the shapes of endothermic reaction cross sections and in deriving accurate thermochemistry (within the stated error limits) for a wide range of systems.²³

At elevated energies, some of the observed reaction cross sections decline with increasing energy. This can be because of dissociation of the product ion or competition with other product channels. These cross sections are reproduced at high energies by using a model for product dissociation that makes a simple statistical assumption within the constraints of angular momentum conservation.²⁴ The model is controlled by two parameters: p , which is an adjustable parameter, and E_D , which is the energy at which the product begins to decompose or competition begins.

Derivation of Bond Energies. The threshold energy, E_0 , for a reaction like process 2 is converted to bond energies by using eq 3. This expression assumes that there are no activation barriers in excess

(22) Chesnavich, W. J.; Bowers, M. T. *J. Phys. Chem.* **1989**, *79*, 900.(23) Armentrout, P. B. In *Advances in Gas Phase Ion Chemistry*; Adams, N. G., Babcock, L. M., Eds.; JAI: Greenwich, CT, 1992; Vol. 1, p 83.(24) Weber, M. E.; Elkind, J. L.; Armentrout, P. B. *J. Chem. Phys.* **1986**, *84*, 1521.(16) Chantry, P. J. *J. Chem. Phys.* **1971**, *55*, 2746.(17) Ervin, K. M.; Armentrout, P. B. *J. Chem. Phys.* **1987**, *86*, 2659.(18) Clemmer, D. E.; Chen, Y. M.; Khan, F. A.; Armentrout, P. B. *J. Phys. Chem.* **1994**, *98*, 6522.(19) Haynes, C. L.; Armentrout, P. B. *Organometallics* **1994**, *13*, 3480.(20) Sunderlin, L. S.; Armentrout, P. B. *J. Phys. Chem.* **1988**, *92*, 1209.(21) van Koppen, P. A. M.; Kemper, P. R.; Bowers, M. T. *J. Am. Chem. Soc.* **1992**, *114*, 10941.

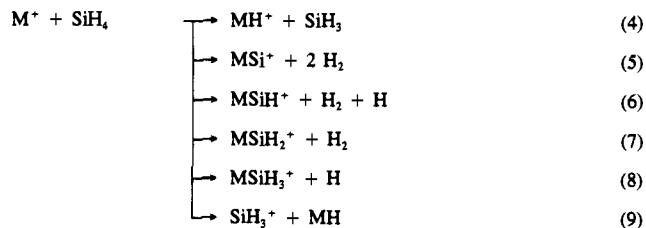


$$D_0(M^+-B) = \Delta_f H_0(B) + \Delta_f H_0(C) - \Delta_f H_0(BC) - E_0 \quad (3)$$

of the endothermicity of the reaction. This assumption is generally reasonable for ion-molecule reactions and has been explicitly tested on a number of occasions.²³ The required literature thermochemistry for the silicon species is listed in Table 2.

Results

Atomic transition metal ions are observed to react with silane according to processes 4–9, where M can refer to Fe, Co, or Ni. The $MSiH_4^+$ adduct was not observed in any system, establishing that its cross sections are below 0.01 \AA^2 .



There are two complexities associated with analyzing the cross sections for these systems. First, because silicon in natural abundance exists as ^{28}Si (92.27%), ^{29}Si (4.68%), and ^{30}Si (3.05%) isotopes, the results obtained for a given m/z ratio can represent several product species. This is straightforward to account for, and the cross sections presented here are total cross sections for all isotopes of a single chemical species.²⁵ Second, in order to transmit ions efficiently, mass resolution is sometimes sacrificed, leading to overlap of signals from adjacent masses. In the present study, cross sections were measured under high-resolution conditions to determine the relative intensity of the products and under low mass resolution to verify efficient product collection.

Ni⁺ and Co⁺ + SiH₄. Product ion cross sections for the reaction of silane with ground state Ni⁺ (a^2D , $3d^9$) and Co⁺ (a^3F , $3d^8$) produced in the DC/FT source are shown as a function of translational energy in Figures 1 and 2, respectively. Formation of $MSiH_2^+ + H_2$ in reaction 7 is the dominant process at low energies. At higher energies, reaction 9, formation of $SiH_3^+ + MH$, dominates the reactivity for M = Ni, and reaction 4, formation of $MH^+ + SiH_3$, dominates the reactivity for M = Co. The $MSiH_2^+$ cross section declines rapidly above ~ 1.5 eV, and the cross section for MSi^+ increases concomitantly, demonstrating that these processes are coupled. Reactions 6 and 8, formation of $MSiH^+ + H_2 + H$ and $MSiH_3^+ + H$, respectively, occur at higher energies and are relatively inefficient. The smooth appearance of the sum of these two cross sections suggests that these two products are closely coupled.

When Co⁺ reactant ions are generated in the DC/FT (no methane in the flow) and SI sources, the cross section for formation of $CoSiH_2^+$ at the lowest energies increases and an exothermic feature appears in the $CoSi^+$ cross section. The SI results are consistent with those of Kang *et al.*, who observed

(25) For example, in the case of $^{56}\text{Fe}^+$, the product at m/z 85 can be due to $\text{Fe}^{28}\text{SiH}^+$ and $\text{Fe}^{29}\text{Si}^+$. The cross section for $\text{Fe}^{29}\text{Si}^+$ is calculated by taking the cross section for m/z 84 (due exclusively to $\text{Fe}^{28}\text{Si}^+$) and scaling it by the $^{28}\text{Si}:^{29}\text{Si}$ isotope ratio, 0.051. Subtraction of this cross section from the m/z 85 cross sections yields the cross section due entirely to $\text{Fe}^{28}\text{SiH}^+$. A similar procedure can then be followed for the m/z 86 (due to $\text{Fe}^{28}\text{SiH}_2^+$, $\text{Fe}^{29}\text{SiH}^+$, and $\text{Fe}^{30}\text{Si}^+$) and m/z 87 (due to $\text{Fe}^{28}\text{SiH}_3^+$, $\text{Fe}^{29}\text{SiH}_2^+$, and $\text{Fe}^{30}\text{SiH}^+$) cross sections. The cross sections for $\text{Fe}^{28}\text{SiH}_x^+$ product ions are then scaled by 1.084 (accounting for the natural abundance of ^{28}Si) to yield the results presented here for a single chemical species. This same general procedure was used for all three metal systems.

Table 2. Heats of Formation and Ionization Energies at 0 K

species	$\Delta_f H_0$, eV	IE, eV
H	2.239 ^a	
SiH ₄	0.46 (0.02) ^a	
SiH ₃	2.14 (0.03) ^b	8.135 (0.005) ^c
SiH ₂	2.85 (0.07) ^d	
SiH	3.92 (0.04) ^e	
Si	4.66 (0.03) ^f	
C ₂ H ₆	-0.707 (0.004) ^g	
(CH ₃) ₂ SiH ₂	-0.75 (0.08) ^g	
FeH		7.28 (0.07) ^h 7.31 (0.07) ⁱ
CoH		7.74 (0.08) ^h 7.86 (0.07) ⁱ
NiH		8.40 (0.12) ^h 8.50 (0.10) ⁱ

^a Reference 72. ^b Seetula, J. A.; Feng, Y.; Gutman, D.; Seakins, P. W.; Pilling, M. J. *J. Phys. Chem.* **1991**, *95*, 1658. The 0 K value given above has been converted from a $\Delta_f H_{298}$ value by using a calculated enthalpy change for SiH₃ of $H(298) - H(0) = 0.106$ eV and elemental enthalpy changes from ref 72. The enthalpy change accounts for the translational, rotational, and vibrational heat capacities but not the electronic, as the necessary molecular information is not available. Vibrational frequencies are taken from the following: Ho, P.; Coltrin, M. E.; Binkley, J. S.; Melius, C. F. *J. Phys. Chem.* **1985**, *89*, 4647. ^c Johnson, R. D.; Tsai, B. P.; Hudgens, J. W. *J. Chem. Phys.* **1989**, *91*, 3340. ^d Frey, H. M.; Walsh, R.; Watts, I. M. *J. Chem. Soc., Chem. Commun.* **1986**, 1189. The 0 K value given above has been converted from a $\Delta_f H_{298}$ value by using a calculated enthalpy change for SiH₂ of $H(298) - H(0) = 0.104$ eV (see footnote b) and elemental enthalpy changes from ref 72. Vibrational frequencies are taken from the following: Fredlin, L.; Hauge, R. H.; Kafafi, Z. H.; Margrave, J. L. *J. Chem. Phys.* **1985**, *82*, 3542. ^e Berkowitz, J.; Ruscic, B. In *Vacuum Ultraviolet Photoionization and Photodissociation of Molecules and Clusters*; Ng, C. Y., Ed.; World Scientific: Singapore, 1991; pp 1–41. The 0 K value given above has been converted from a $\Delta_f H_{298}$ value by using an enthalpy change for SiH of $H(298) - H(0) = 0.096$ eV and elemental enthalpy changes from ref 72. ^f Fisher, E. R.; Kickel, B. L.; Armentrout, P. B. *J. Phys. Chem.* **1993**, *97*, 10204. ^g Doncaster, A. M.; Walsh, R. *J. Phys. Chem.* **1979**, *83*, 3037. The $\Delta_f H_{298}$ value given in this reference is converted to a 0 K heat of formation by using the enthalpy change of propane, which we assume is similar to (CH₃)₂SiH₂, and elemental enthalpy changes from ref 72. ^h Reference 37. ⁱ Recommended values obtained in the present study (see text).

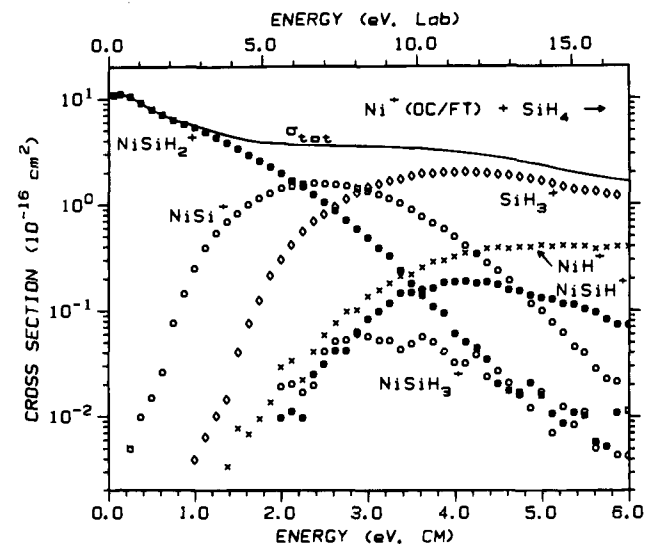


Figure 1. Variation of product cross sections for the reaction of Ni⁺ (produced in the dc-discharge/flow tube source) with silane as a function of translational energy in the laboratory frame (upper scale) and the center-of-mass frame (lower scale).

only exothermic formation of $CoSiH_2^+ + H_2$ with an absolute cross section somewhat larger than that measured here.⁶

Fe⁺ + SiH₄. Figure 3 shows results for Fe⁺ produced in the DC/FT source, predominately ground state (a^6D , $4s3d^6$) with a small ($\sim 2\%$) contribution from the first excited state (a^4F , $3d^7$). At the lowest energies, the $FeSiH_2^+$ cross section increases

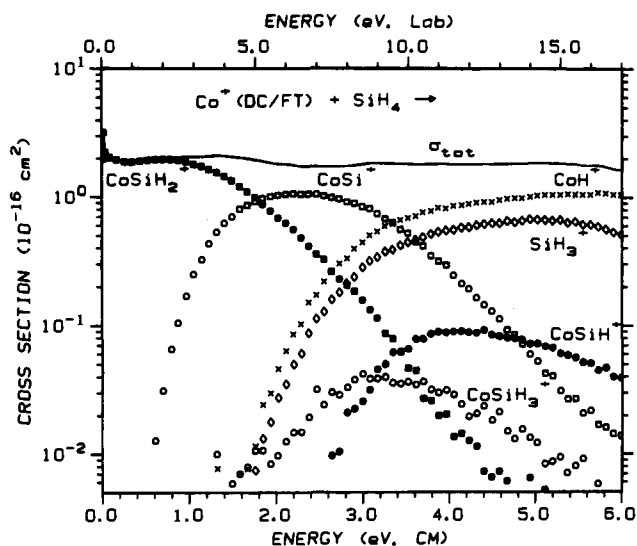


Figure 2. Variation of product cross sections for the reaction of Co^+ (produced in the dc-discharge/flow tube source) with silane as a function of translational energy in the laboratory frame (upper scale) and the center-of-mass frame (lower scale).

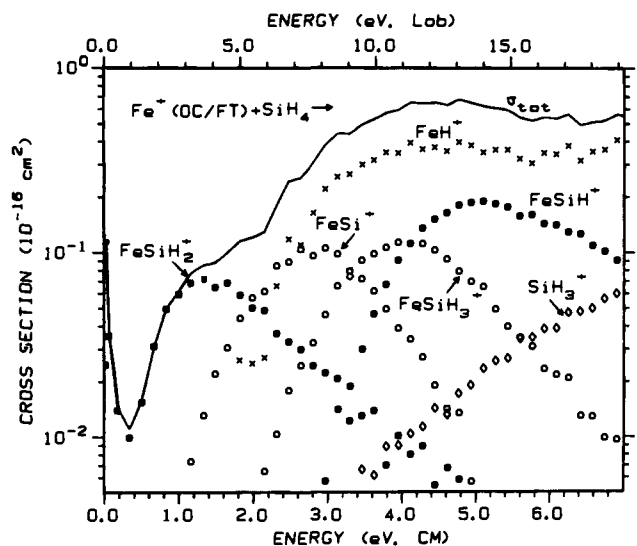


Figure 3. Variation of product ion cross sections for the reaction of Fe^+ (produced in the dc-discharge/flow tube source) with silane as a function of translational energy in the laboratory frame (upper scale) and center-of-mass frame (lower scale).

with decreasing energy, a feature that changes magnitude as the amount of O_2 in the flow source is varied (while no other changes in the cross sections are observed). All the same reactions observed in the Co^+ and Ni^+ systems are observed here; however, the relative amounts of the products differ substantially. Although FeSiH_2^+ is the dominant product at the lowest energies, its maximum cross section is smaller than all the other product cross sections except SiH_3^+ , while the maxima in the CoSiH_2^+ and NiSiH_2^+ cross sections are larger than any other product cross sections. Also, production of FeSiH^+ and FeSiH_3^+ in reactions 6 and 8 are larger contributors to the total reactivity than the same species in the Co^+ and Ni^+ systems.

Figure 4 shows results for Fe^+ produced in the SI source at a filament temperature of $2300 \pm 100 \text{ K}$, where the beam consists of $78.3 \pm 1.0\% \text{ Fe}^+$ ($a^6\text{D}$) and $21.3 \pm 1.0\% \text{ Fe}^+$ ($a^4\text{F}$), Table 1. Kang *et al.* investigated the reaction of silane with Fe^+ produced in a SI source and observed no reaction at 0.5 eV.⁶ We do observe a small reactivity, $\leq 0.1 \text{ \AA}^2$, but this is below the detection limit of the previous experiment. Com-

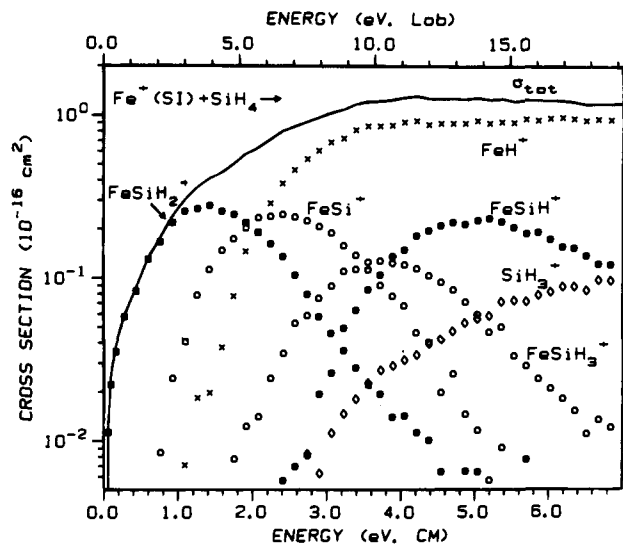


Figure 4. Variation of product ion cross sections for the reaction of Fe^+ (produced in the surface ionization source) with silane as a function of translational energy in the laboratory frame (upper scale) and center-of-mass frame (lower scale).

parison of Figures 3 and 4 shows that the reactivity of Fe^+ (SI) is greater than that observed for Fe^+ (DC/FT) and that the threshold energies for Fe^+ (SI) have shifted to lower energies by 0.2–0.4 eV. The exothermic feature in the FeSiH_2^+ cross section of Figure 3 is not found in Figure 4. This indicates that this feature must be due to reactions of excited states lying higher than the $a^4\text{F}$ (Table 1), consistent with the observation that these states are quenched by adding O_2 to the flow tube. This feature can be reproduced nicely by $\sim 0.02\%$ of the collision cross section, σ_{LGS} ,^{26–28} indicating that a very small population of these excited states can account for the observed reactivity. Comparison of Figures 2 and 4 reveals that the overall reactivity of Fe^+ (SI) closely resembles the reactivity for ground state Co^+ . Both the difference in product distribution and the shift in threshold energies are consistent with contributions from the $a^4\text{F}$ state of Fe^+ (Table 1) to the SI data.

To explicitly examine the relative contributions of the Fe^+ ($a^4\text{F}$) and Fe^+ ($a^6\text{D}$) states, we extract state-specific cross sections for reaction with silane. The conversion of the raw SI and DC/FT data to state-specific data is relatively straightforward. At $2300 \pm 100 \text{ K}$, the SI ion beam consists of $78.3 \pm 1.0\% \text{ Fe}^+$ ($a^6\text{D}$), $21.3 \pm 1.0\% \text{ Fe}^+$ ($a^4\text{F}$), and 0.4% of higher lying states which we ignore. To extrapolate to the state-specific behavior of the Fe^+ ($a^4\text{F}$) excited electronic state, the DC/FT data (assumed to be 98% $a^6\text{D}$) is scaled by a factor of 0.783 and subtracted from the SI data. The remaining cross section is divided by 0.213 to account for the percentage of $a^4\text{F}$ in the reactant beam. We then use the state-specific $a^4\text{F}$ cross sections to correct the DC/FT data for the 2% contribution from this excited state in a similar manner. The exothermic feature in the FeSiH_2^+ (DC/FT) cross section is also removed by subtracting 0.02% σ_{LGS} . State-specific cross sections for pure Fe^+ ($a^6\text{D}$) and Fe^+ ($a^4\text{F}$) derived in this fashion are shown in Figures 5 and 6.

(26) Gioumousis, G.; Stevenson, D. P. *J. Chem. Phys.* **1958**, *29*, 292.

(27) The LGS (Langevin–Gioumousis–Stevenson) model for collision cross sections of ion–molecule reactions at low energies is given by $\sigma_{\text{LGS}} = \pi e(2\alpha/E)^{1/2}$, where e is the electron charge, α is the polarizability of the target molecule, and E is the relative kinetic energy of the reactants.

(28) The value used here for $\alpha(\text{SiH}_4) = 4.62 \text{ \AA}^3$ is recommended by Haaland: Haaland, P. Technical Report No. AFWAL-TR-88-2043; Aero Propulsion Lab: Air Force Wright Aeronautical Lab, Wright-Patterson Air Force Base, Ohio, 1988.

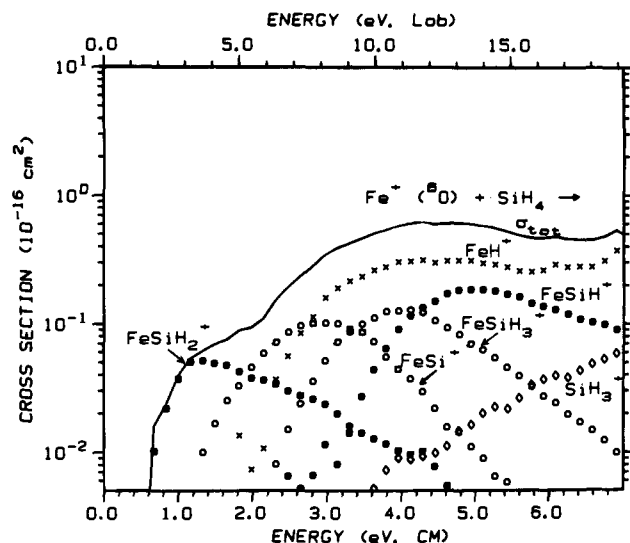


Figure 5. Variation of product cross sections as a function of translational energy for the reaction of state-specific Fe^+ (a^6D) with silane (see text). The upper scale is the laboratory frame, and the lower scale is the center-of-mass frame.

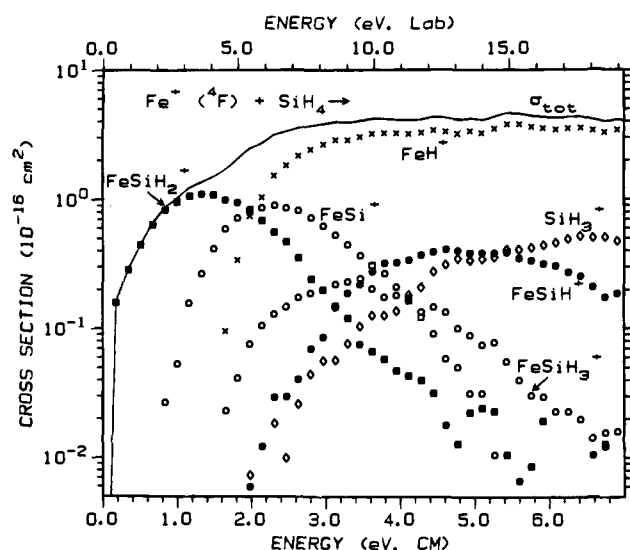


Figure 6. Variation of product cross sections as a function of translational energy for the reaction of state-specific Fe^+ (a^4F) with silane (see text). The upper scale is the laboratory frame, and the lower scale is the center-of-mass frame.

Comparison of the state-specific data shows that ground state Fe^+ (a^6D) exhibits a different product distribution and is less reactive than excited state Fe^+ (a^4F). The excited state cross sections for reactions 4, 5, 7, and 9 increase by an order of magnitude, while those for reactions 6 and 8 increase by a factor of ~ 3 . Reactions of Fe^+ (a^4F) with dihydrogen,¹¹ methane, ethane, and propane¹² show similar enhancements in reactivity compared to ground state Fe^+ (a^6D). Comparison of Figures 2 and 6 shows that the distribution of products and efficiency of reaction for excited state Fe^+ (a^4F) closely resemble those of ground state Co^+ (a^3F). As is discussed below, this correspondence is reasonable and helps to confirm that the former cross sections are sensible in shape and magnitude.

Thermochemistry

The threshold regions of the cross sections for Fe^+ (a^4F), Co^+ (DC/FT), and Ni^+ (DC/FT) data are analyzed by using eq 1. These analyses are summarized in Table 3, and in all cases, the

model of eq 1 accurately reproduces the experimental results. Although the results are not listed in Table 3, the Fe^+ cross sections for a^6D , SI, and DC/FT data sets were also analyzed to ensure that they were consistent with the a^4F thresholds. In general, we consider the analysis of the a^4F state-specific cross sections to give the most reliable thermochemical information. The a^4F cross sections are large and tend to rise more quickly from threshold, making the exact determinations of these thresholds more precise and accurate. Analysis of the SI and DC/FT data is complicated by the drastically different reactivities of the two electronic states of Fe^+ .

Measured threshold energies, E_0 , listed in Table 3 are combined with literature thermochemistry (Table 2) in eq 3 to determine 0 K bond energies for M^+-SiH_x ($x = 0-3$) for $\text{M} = \text{Fe}, \text{Co},$ and Ni . These bond energies are listed in Table 4. Few M^+-SiH_x bond energies have been determined previously. The only experimentally determined M^+-SiH_x bond energies related to the present study were determined by Kang *et al.*⁶ They observed that the reaction of dimethylsilane with Fe^+ (resulting in formation of $\text{FeSiH}_2^+ + \text{C}_2\text{H}_6$) is endothermic, placing an upper limit of 2.89 ± 0.11 eV²⁹ on the Fe^+-SiH_2 bond energy. This upper limit agrees with the 1.88 ± 0.09 eV bond energy derived in the present study. They also observed that Co^+ and Ni^+ exothermically dehydrogenate silane and endothermically eliminate ethane from dimethylsilane. These two reactions place the M^+-SiH_2 ($\text{M} = \text{Co}$ and Ni) bond energies at 2.66 ± 0.34 eV.²⁹ We also find that the dehydrogenation of silane by Ni^+ is exothermic, yielding $D_0(\text{Ni}^+-\text{SiH}_2) \geq 2.39 \pm 0.07$ eV, but we believe the dehydrogenation of silane is endothermic for ground state Co^+ , and thus we get a lower Co^+-SiH_2 bond energy of 2.25 ± 0.08 eV. To verify our conclusion, we note that addition of methane to the flow¹⁹ in the DC/FT source quenches excited states of Co^+ and results in the cross section behavior shown in Figure 2. At the lowest energies, the CoSiH_2^+ cross section increases with decreasing energy, indicative of an exothermic reaction and consistent with the observations of Kang *et al.* Approximately 1% of σ_{LGS} accounts for this low energy reactivity.²⁶⁻²⁸ We believe that the threshold for dehydrogenation of silane by Co^+ to be sufficiently small that states higher in energy than the a^3F_3 , which account for 3% of the beam at 800 K, react exothermically to form CoSiH_2^+ . We are able to reproduce the energy behavior of the CoSiH_2^+ cross section by combining a 1% contribution of σ_{LGS} with a model for an endothermic process with $E_0 = 0.14$ eV (an energy lower than the excitation energy of all states but the a^3F_4 ground and a^3F_3 spin-orbit levels).³⁰ Kang *et al.* studied this reaction at energies above 0.2 eV with Co^+ generated by SI at 2560 K, leading to 78% a^3F ground state (average electronic energy of 0.056 eV), 22% of the a^5F (0.487 eV), and $<1\%$ b^3F (1.28 eV). The higher percentage of excited states present in the beam combined with an inability to examine very low kinetic energies led Kang *et al.* to believe that dehydrogenation of silane by Co^+ is exothermic. The theoretical calculations of Musaev *et al.*⁹ on metal methylidene and silylene complexes provide a binding energy $D_e(\text{Co}^+-\text{SiH}_2) = 2.67$ eV, which we convert to $D_0(\text{Co}^+-\text{SiH}_2) = 2.52$ eV, in reasonable agreement with the present results.³¹

Bond energies having been derived for the various MSiH_x^+ species (Table 4), the energy dependencies of the individual

(29) Reference 6 cites values for $D(\text{Fe}^+-\text{SiH}_2) < 3.11$ eV, $D(\text{Co}^+-\text{SiH}_2) = 2.86 \pm 0.26$ eV, and $D(\text{Ni}^+-\text{SiH}_2) = 2.86 \pm 0.26$ eV at a temperature of 298 K. To compare to the present results, these bond energies have been changed to 0 K values by using the heats of formation listed in Table 2.

(30) Sugar, J.; Corliss, C. *J. Phys. Chem. Ref. Data* **1978**, *7*, 158.

(31) The zero-point energy of Co^+-SiH_2 is calculated by using frequencies given in ref 9.

Table 3. Summary of Optimum Parameters in Eq 1^a

reaction	E ₀ , eV	n	σ ₀	p	E _D , eV
Fe ⁺ (a ⁴ F) ^b + SiH ₄ →					
FeH ⁺ + SiH ₃	1.85 (0.05)	1.3 (0.1)	5.84 (0.60)		
FeSi ⁺ + 2H ₂	1.33 (0.09)	1.4 (0.4)*	1.76 (0.13)	2, 3	2.7 (0.1)
FeSiH ⁺ + H ₂ + H	3.06 (0.12)	1.2 (0.4)*	1.12 (0.14)	1, 2	5.0 (0.2)
FeSiH ₂ ⁺ + H ₂	0.51 (0.05)	1.6 (0.2)	1.44 (0.19)	2	2.1 (0.1)
FeSiH ₃ ⁺ + H	2.02 (0.10)	1.2 (0.4)*	0.51 (0.08)	2, 3	3.6 (0.2)
SiH ₃ ⁺ + FeH	2.59 (0.04)	1.7 (0.1)	0.33 (0.05)		
Co ⁺ (DC/FT) ^c + SiH ₄ →					
CoH ⁺ + SiH ₃	2.02 (0.02)	1.7 (0.1)	1.03 (0.13)		
CoSi ⁺ + 2H ₂	0.95 (0.06)	1.2 (0.2)	1.92 (0.15)	2	2.4 (0.1)
CoSiH ⁺ + H ₂ + H	2.67 (0.15)	1.6 (0.7)*	0.27 (0.06)	1, 2	4.1 (0.2)
CoSiH ₂ ⁺ + H ₂	0.14 (0.04)	1.0 (0.1)	1.91 (0.07)	2	2.0 (0.1)
CoSiH ₃ ⁺ + H	1.96 (0.13)	1.3 (0.7)*	0.11 (0.03)	1, 2	3.0 (0.2)
SiH ₃ ⁺ + CoH	2.00 (0.07)	1.6 (0.2)	0.79 (0.24)		
Ni ⁺ (DC/FT) ^c + SiH ₄ →					
NiH ⁺ + SiH ₃	2.32 (0.16)	1.4 (0.4)*	0.44 (0.09)		
NiSi ⁺ + 2H ₂	0.86 (0.05)	1.5 (0.2)	2.10 (0.18)	3	2.7 (0.1)
NiSiH ⁺ + H ₂ + H	2.32 (0.14)	1.5 (0.5)*	0.36 (0.10)	2	4.0 (0.2)
NiSiH ₂ ⁺ + H ₂	0.00 ^d	0.5 (0.1)	5.12 (0.70)	2	2.3 (0.1)
NiSiH ₃ ⁺ + H	2.01 (0.11)	1.4 (0.6)*	0.32 (0.05)	1, 2	3.0 (0.2)
SiH ₃ ⁺ + NiH	1.79 (0.06)	1.4 (0.2)	3.02 (0.45)		

^a Uncertainties are in parentheses. Asterisks represent those analyses where the value of *n* is fixed over the indicated range (see text). ^b Fe⁺ (4F) state-specific cross sections are analyzed without a distribution of electronic states. Once the threshold has been determined with the model of eq 1, the average electronic energy of Fe⁺ at 2300 K (0.284 eV) is included to give E₀, the threshold for reaction of Fe⁺ (a⁴D_{9/2}) at 0 K. ^c Ions generated in the dc-discharge/flow tube source. ^d Exothermic reaction.

Table 4. Experimental Bond Energies at 0 K, eV^a

L	D(Fe ⁺ -L)	D(Co ⁺ -L)	D(Ni ⁺ -L)
H	2.12 (0.06) ^b	1.98 (0.06) ^c	1.68 (0.08) ^c
C	4.1 (0.3) ^d	3.9 (0.3) ^d	
CH	4.4 (0.3) ^d	4.3 (0.3) ^d	
CH ₂	3.54 (0.04) ^e	3.29 (0.05) ^e	3.17 (0.04) ^e
CH ₃	2.37 (0.05) ^e	2.10 (0.04) ^e	1.94 (0.06) ^e
Si	2.87 (0.09)	3.25 (0.07)	3.34 (0.07)
SiH	2.63 (0.13)	3.03 (0.16)	3.38 (0.15)
SiH ₂	1.88 (0.09)	2.29 (0.07)	≥2.39 (0.07)
	<2.89 (0.11) ^f	2.66 (0.34) ^f	2.66 (0.34) ^f
		2.52 ^g	
SiH ₃	1.90 (0.09)	1.96 (0.13)	1.91 (0.12)

^a Unless otherwise noted, values are taken from the present study. Uncertainties are 1σ and are listed in parentheses. Bond energies for MXH_x⁺ (X = C or Si, x = 1–3) represent the energy difference between the ground state of this species (of unknown structure) and the indicated dissociation products. ^b Elkind, J. L.; Armentrout, P. B. *J. Am. Chem. Soc.* **1986**, *108*, 2765; *J. Phys. Chem.* **1986**, *90*, 5736. ^c Elkind, J. L.; Armentrout, P. B. *J. Phys. Chem.* **1986**, *90*, 6576. ^d Hettich, R. L.; Freiser, B. S. *J. Am. Chem. Soc.* **1986**, *108*, 2537. The temperature to which this bond energy corresponds is unknown. ^e Reference 37. ^f Reference 6. Converted to 0 K as discussed in the text. ^g Converted from the D_c value given in ref 9.

product cross sections can now be analyzed in more detail. This is done in the following sections.

MH⁺ and SiH₃⁺. Formation of MH⁺ + SiH₃ is thermodynamically favored over SiH₃⁺ + MH⁺ for M = Fe and Co because the ionization energies (IEs) of FeH and CoH are lower than IE(SiH₃) (Table 2). In contrast, IE(NiH) is higher than IE(SiH₃); therefore, we find formation of SiH₃⁺ + NiH to be favored over NiH⁺ + SiH₃. Furthermore, formation of SiH₃⁺ + MH is a simple hydride ion (H⁻) transfer from SiH₄ to M⁺ (although the mechanism may be more complex). Such a reaction may occur most readily when the metal ion has an empty 4s orbital,³² because this avoids repulsive interactions between the 4s electron and the pair of H⁻ electrons. The ground state of Fe⁺ (a⁶D, 4s3d⁶), unlike the ground states of Co⁺ (a³F, 3d⁸) and Ni⁺ (a²D, 3d⁹), has an occupied 4s orbital. This combination of thermochemical and electronic effects

explains why the efficiency for production of the silyl cation is Ni⁺ (3d⁹) > Co⁺ (3d⁸) > Fe⁺ (a⁴F, 3d⁷) > Fe⁺ (a⁶D, 4s3d⁶).

The measured thresholds for MH⁺ + SiH₃ formation, Table 3, are consistent with calculated values of 1.80 ± 0.07, 1.94 ± 0.07, and 2.24 ± 0.09 eV (Tables 2 and 3) for ground state Fe⁺, Co⁺, and Ni⁺, respectively. This helps to confirm that the DC/FT source produces predominantly ground state Co⁺ and Ni⁺ and that the extracted Fe⁺(a⁴F) cross section is reasonable. The thresholds for the competing SiH₃⁺ + MH formation, reaction 9, for M = Fe, Co, and Ni are slightly lower than the calculated literature thresholds of 2.66 ± 0.06, 2.34 ± 0.06, and 1.98 ± 0.09 eV, respectively. In previous work, we have evaluated reactions of propane, cyclopropane, butane, cyclopentane, and acetaldehyde³³ with Fe⁺ and ethane, propane, isobutane,³⁴ and cyclopropane³⁵ and Co⁺ and Ni⁺ to determine D(M–H). A weighted average³⁶ of these results (converted to 0 K bond energies) yields D₀(Fe–H) = 1.49 ± 0.04 eV, D₀(Co–H) = 1.86 ± 0.05 eV and D₀(Ni–H) = 2.45 ± 0.08 eV.³⁷ Thresholds determined in the present study yield D₀(Fe–H) = 1.56 ± 0.04 eV, D₀(Co–H) = 2.05 ± 0.04 eV, and D₀(Ni–H) = 2.63 ± 0.07 eV. The FeH bond energy is in good agreement, but the CoH and NiH bond energies are higher than the previous average, although comparable to the highest values we have previously derived: D₀(Co–H) = 2.02 ± 0.19 eV from the isobutane system and D₀(Ni–H) = 2.62 ± 0.18 eV from the cyclopropane system. Because the present systems involve a near-resonant charge transfer that minimizes the competition between SiH₃⁺ and MH⁺ formation, they should provide a reliable determination of the threshold. Such competition would yield M–H bond energies that are too low, and this probably explains much of the spread in values obtained in previous work. Other recent studies of the reactions of water³⁸ and propene¹⁹

(33) Schultz, R. H.; Armentrout, P. B. *J. Chem. Phys.* **1991**, *94*, 2262.

(34) Georgiadis, R.; Fisher, E. R.; Armentrout, P. B. *J. Am. Chem. Soc.* **1989**, *111*, 4251.

(35) Fisher, E. R.; Armentrout, P. B. *J. Phys. Chem.* **1990**, *94*, 1674.

(36) Taylor, J. R. *An Introduction to Error Analysis*; University Science: Mill Valley, 1982.

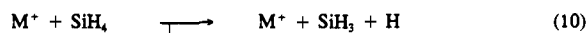
(37) Armentrout, P. B.; Kickel, B. L. *Organometallic Ion Chemistry*; Freiser, B. S., Ed.; Kluwer: Dordrecht, in press.

(38) Chen, Y. M.; Clemmer, D. E.; Armentrout, P. B. *J. Am. Chem. Soc.* **1994**, *116*, 7815.

(32) Schultz, R. H.; Elkind, J. L.; Armentrout, P. B. *J. Am. Chem. Soc.* **1988**, *110*, 411.

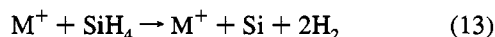
with Co^+ yield $D_0(\text{Co}-\text{H})$ of 1.89 ± 0.06 and 1.83 ± 0.12 eV, respectively. A weighted average³⁶ of all our available values yields $D_0(\text{Fe}-\text{H}) = 1.52 \pm 0.05$ eV, $D_0(\text{Co}-\text{H}) = 1.95 \pm 0.05$ eV, and $D_0(\text{Ni}-\text{H}) = 2.56 \pm 0.11$ eV (where the uncertainties are two standard deviations), which we take as our best values for these bond energies.

MSiH_3^+ and MSiH^+ . As mentioned above, the sums of the cross sections for MSiH_3^+ and MSiH^+ are smooth functions of energy, implying that these processes are closely related (Figures 1, 2, 5, and 6). Therefore, we believe that the MSiH_3^+ cross sections decline at high energies because the product dehydrogenates to form $\text{MSiH}^+ + \text{H}_2$ in reaction 6. This is consistent with the results of the reactions of silane with Ti^+ , V^+ , and Cr^+ .⁵ Additional evidence for this strong coupling comes from the decline in the MSiH^+ cross sections, which could be due to reactions 10, 11, or 12. The thresholds for reactions 10 and 11



are 3.92 ± 0.04 and 5.70 ± 0.05 eV, respectively, while those for reactions 12 are calculated to be 5.81 ± 0.10 , 5.43 ± 0.08 , and 5.34 ± 0.08 eV for Fe^+ , Co^+ , and Ni^+ , respectively. The dissociation energies, E_D , used to model the MSiH^+ cross sections (Table 3) are most consistent with the decline caused by reaction 10, which depletes the MSiH_3^+ precursor to the MSiH^+ product.

MSiH_2^+ and MSi^+ . In all three metal systems, the sum of the MSiH_2^+ , MSi^+ , MH^+ , and SiH_3^+ cross sections yields a total cross section that varies smoothly with energy, implying that these various products are coupled. Examination of Figures 1, 2, 5, and 6 clearly shows that the initial decline of the MSiH_2^+ is a result of dehydrogenation to form $\text{MSi}^+ + \text{H}_2$, reaction 5. Additional evidence for the coupling between these two products comes from the decline in the MSi^+ cross sections. This could result from reaction 13.



However, this process is not thermodynamically possible until 4.16 ± 0.08 eV, and the MSi^+ cross sections decline well before this energy. Because MSi^+ must be formed by dehydrogenation of the MSiH_2^+ product, the decline in the MSi^+ cross sections is due to depletion of the MSiH_2^+ precursor. This depletion could be caused by dissociation to form $\text{M}^+ + \text{SiH}_2$, which can begin at 2.39 ± 0.07 eV, or by competition with formation of $\text{MH}^+ + \text{SiH}_3$ ($\text{M} = \text{Fe}$ and Co) or $\text{SiH}_3^+ + \text{MH}$ ($\text{M} = \text{Ni}$). The smooth behavior of the sum of the MSiH_2^+ , MSi^+ , MH^+ , and SiH_3^+ product cross sections suggests that the latter is the dominant depletion mechanism. The coupling between these products was also observed for the reactions of silane with Ti^+ , V^+ , and Cr^+ .⁵

Comparison of M^+-CH_x and M^+-SiH_x Bond Energies. Table 4 lists the M^+-SiH_x bond energies measured here and the available M^+-CH_x bond energies. In general, the metal-silicon bond energies are weaker than the metal-carbon energies, consistent with the theoretical calculations of MSiH_2^+ vs MCH_2^+ bond energies by Cundari and Gordon⁸ and Musaev *et al.*⁹

In the past, we have discussed the relationships between the bond energies of metal-carbon and related organic species.^{39,40} The ratios of the bond energies of $D(\text{H}-\text{CH}_3)$, $D(\text{CH}_3-\text{CH}_3)$,

$D(\text{CH}_2=\text{CH}_2)$, $D(\text{CH}\equiv\text{CH})$, and $D(\text{C}-\text{C})$ are 1.0:0.9:1.7:2.2:1.4. These bond energy relationships are consistent with the multiple bonding exhibited by the organic species. The bond energies of $D(\text{M}^+-\text{H})$, $D(\text{M}^+-\text{CH}_3)$, $D(\text{M}^+-\text{CH}_2)$, $D(\text{M}^+-\text{CH})$, and $D(\text{M}^+-\text{C})$ are related as 1.0:1.1:1.7:2.1:1.8 for $\text{M} = \text{Fe}$, 1.0:1.1:2.0:2.2:2.1 for $\text{M} = \text{Co}$, and 1.0:1.2:1.9 for $\text{M} = \text{Ni}$ (where no NiCH^+ or NiC^+ bond energies are known). The general similarities in the organic and metal-carbon relationships are taken to indicate that MH^+ and MCH_3^+ species are singly bonded and that MCH_2^+ , MCH^+ , and MC^+ are multiply bonded.

The bond energies of $D(\text{M}^+-\text{H})$, $D(\text{M}^+-\text{SiH}_3)$, $D(\text{M}^+-\text{SiH}_2)$, $D(\text{M}^+-\text{SiH})$, and $D(\text{M}^+-\text{Si})$ are related as 1.0:0.9:0.9:1.2:1.4 for $\text{M} = \text{Fe}$, 1.0:1.0:1.2:1.5:1.6 for $\text{M} = \text{Co}$, and 1.0:1.1: \geq 1.4:2.0:2.0 for $\text{M} = \text{Ni}$. Direct comparison of the metal-carbon and metal-silicon bond relationships (both relative to MH^+) shows that the metal-silicon single bond is comparable to the metal-carbon single bond for $\text{M} = \text{Fe}$, Co , and Ni . M^+-SiH_x ($x = 0-2$) bond energies are relatively weak compared to the analogous M^+-CH_x ($x = 0-2$) bond energies for $\text{M} = \text{Fe}$ and Co , and data for $\text{M} = \text{Ni}$ are insufficient to make a substantive comparison. These results are consistent with the difficulty that silicon has in forming double bonds and are similar to results for the earlier transition metal ions of Ti^+ , V^+ , and Cr^+ .⁵

To gain insight into the bonding mechanisms of the metal-silicon species, a more valuable comparison is to the silicon-silicon-bonded analogues. The bond energies of $D(\text{H}-\text{SiH}_3)$, $D(\text{SiH}_3-\text{SiH}_3)$,⁴¹ $D(\text{H}_2\text{Si}-\text{SiH}_2)$,⁴² $D(\text{HSi}-\text{SiH})$,⁴³ and $D(\text{Si}-\text{Si})$ ⁴⁴ are related as 1.0:0.8:0.8:1.0:0.8. These silicon-silicon bond energy relationships illustrate the difficulty silicon has in forming multiple bonds because the bond energies do not increase as for the single, double, and triple bonds of the analogous carbon species. Compared to these silicon-silicon bond energy relationships, the metal-silicon relationships are similar for H and SiH_3 ; however, the metal-silicon bond energy relationships then increase for SiH_2 , SiH , and Si ligands. Because the silicon-silicon interactions are covalent, this difference suggests that the bonding between metal ions and SiH_2 , SiH , and Si involves different types of interactions, such as dative bonding. For silylene, this would correspond to the $\text{SiH}_2(^1A_1)$ ground state^{45,46} donating its a_1 lone pair of electrons into an empty metal 4s orbital accompanied by back-donation of a pair of $3d\pi$ electrons from the metal to the empty b_1 orbital on SiH_2 . The bonding of the MSiH_2^+ species is discussed by Cundari and Gordon,⁸ who conclude that the Fe^+-SiH_2 bond may be described by almost equal contributions from this type of dative double bond (20%), a covalent double bond (25%), and (30%) ylide-like bonding, $\text{M}^{2+}-\text{SiH}_2^-$, corresponding to a dative σ -bond and a covalent π bond. They describe the Co^+-SiH_2 bond as largely a dative double bond (55%) with small contributions from ylide-like (22%) and covalent double bonding (8%). The bonding of Ni^+-SiH_2 is described by still larger contributions of dative double bonding (65%) and small contributions from ylide-like (25%) and covalent double bonding (5%). Dative bonding contributions to the interactions of metal ions with $\text{SiH}(^2\Pi)$ and $\text{Si}(^3P)$ also seem likely.

(41) $\Delta_f H_0(\text{Si}_2\text{H}_6) = 1$ eV taken from the following: Lias, S. G.; Bartmess, J. E.; Liebman, J. F.; Holmes, J. L.; Levin, R. D.; Mallar, W. G. *J. Phys. Chem. Ref. Data* **1988**, *17*, No. 1.

(42) Kutzelnigg, W. *Angew. Chem., Int. Ed. Engl.* **1984**, *23*, 272.

(43) Ruscic, B.; Berkowitz, J. *J. Chem. Phys.* **1991**, *95*, 2416.

(44) Huber, K. P.; Herzberg, G. *Molecular Spectra and Molecular Structure Constants of Diatomic Molecules*; Van Nostrand Reinhold Company: New York, 1979 and references therein.

(45) Berkowitz, J.; Greene, J. P.; Cho, H. *J. Chem. Phys.* **1987**, *86*, 1235.

(46) Bauschlicher, C. W.; Taylor, P. R. *J. Chem. Phys.* **1987**, *86*, 1420.

(39) Aristov, N.; Armentrout, P. B. *J. Am. Chem. Soc.* **1984**, *106*, 4065.

(40) Armentrout, P. B. In *Selective Hydrocarbon Activation: Principles and Progress*; Davies, J. A., Watson, P. L., Greenberg, A., Liebman, J. F., Eds.; VCH: New York, 1990; pp 467-533.

Another way to think about these bond energies is to compare the absolute values as a function of metal. Table 4 shows that the M⁺-H, M⁺-CH₃, and M⁺-CH₂ bond energies decrease from M = Fe to Co to Ni, consistent with the increasing promotion energy needed to allow these metals to form covalent bonds. This pattern has been discussed in detail previously.^{37,47,48} In contrast, the M⁺-SiH₃ bond energies are approximately constant for all three metals, while the M⁺-SiH_x (x = 0-2) bond energies increase from M = Fe to Co to Ni. A comparable increase is also observed for the bond energies of these metal ions with H₂O,⁴⁹ interactions that must be dative bonding. This comparison lends credence to the conclusion reached above that the SiH₂, SiH, and Si ligands bond to the metal ions largely through dative interactions. The constancy of the M⁺-SiH₃ bond energies is not clearly understood, because the trends do not appear to correspond to either a pure covalent or a pure dative interaction.

Another complication in understanding the trends in these bond energies is the possibility that some of the hydrogen atoms are bonded directly to the metal, e.g., H-M-SiH₂⁺ instead of M-SiH₃⁺, or that they bridge the metal and silicon atoms. The first possibility cannot be ruled out entirely, although it seems unlikely because the metal-hydrogen bond energies (Table 4) are all weaker than even the weakest silicon-hydrogen bond, D(H₂Si-H) = 2.95 eV (Table 2). In agreement with this, Ferhati and Ohanessian find that Y⁺-SiH₂ is considerably more stable than HY⁺-SiH.¹⁰ Bridging hydrogens are known to be important in Si₂H₄⁺, Si₂H₄, and Si₂H₂ species.⁵⁰⁻⁵² In the Si₂H₄ case, the ethene-like structure is calculated to be the ground state structure but the double-bridged isomer, HSi(H)₂SiH, is a local minimum about 1 eV higher in energy. In the Si₂H₂ case, calculations indicate that the monobridged Si(H)SiH, disilavinylidene (H₂SiSi), and *trans*-HSiSiH isomers all lie within 0.9 eV of the ground state double-bridged Si(H₂)Si structure. The theoretical studies of Ferhati and Ohanessian are consistent with this possibility in that they find the doubly bridged Y(H)₂Si⁺ structure has a comparable stability to the Y⁺-SiH₂ structure.¹⁰ Kang *et al.* performed collision-induced dissociation (CID) on CoSiH₂⁺ and found that it dissociated almost exclusively to Co⁺ + SiH₂ (82.0%). The remaining CID products are CoSi⁺ + H₂ (14.5%) and CoSiH⁺ + H (3.5%). These results suggest that the structure of CoSiH₂⁺ can be formulated as a cobalt-silylene complex, M⁺-SiH₂, and not H-M⁺-SiH or (H₂)M⁺-Si. However, the presence of bridged structures cannot be ruled out by this CID result. The present results also cannot be used to ascertain which of the MH_xSi⁺ structures or bonding mechanisms may be the most important.

Discussion

Comparison to Ti⁺, V⁺, and Cr⁺. Previously we have investigated the reactions of silane with Ti⁺, V⁺, and Cr⁺.⁵ Of the early ground state metals, titanium reacts most efficiently followed by vanadium and chromium. As we move across the periodic table, Fe⁺ (a⁶D) is ~3 times more reactive than ground state Cr⁺. The efficiency of reaction with silane then increases for Fe⁺ (a⁴F) to Co⁺ to Ni⁺, which reacts more than an order of magnitude more efficiently than titanium. As is the case

with Fe⁺, low-spin excited states of Ti⁺, V⁺, and Cr⁺ are all more reactive with silane than the high-spin ground states.⁵

The M⁺-SiH_x bond energies decrease in strength from Ti⁺ to V⁺ to Cr⁺ and then increase in strength for Fe⁺ to Co⁺ to Ni⁺. The M⁺-CH_x (x = 2, 3) bond energies follow the same trend from titanium to iron; however, the cobalt- and nickel-carbon bond energies then decrease. The increase of the cobalt- and nickel-silicon bond energies suggests a different bonding mechanism for these species compared to the carbon analogues. As discussed above, dative contributions to the bonding of the cobalt- and nickel-silicon species probably explain the differences between the periodic trends in metal-carbon and metal-silicon bond strengths.

Comparison with the Reactions of Fe⁺, Co⁺, and Ni⁺ with Methane. The effect that substitution of Si for C can have in organotransition metal bonding can be investigated by comparing our present results to beam studies of the reactivity of methane with Fe⁺, Co⁺, and Ni⁺.^{12,53-55} The reactions with methane result in significantly different product distributions than those observed in the present results. The most dramatic difference is the dominance of MH⁺ + CH₃ over all other observed processes, MCH₃⁺ (for M = Fe, Co, and Ni) and MCH₂⁺ (for M = Co and Ni). No CH₃⁺ + MH products are observed, and only small amounts of MCH⁺ and MC⁺ products are observed in the case of M = Co.⁵⁴ The overall reactivity of the silane systems is greater with total cross sections approximately 5, 3, and 2 times greater for Fe⁺ (a⁶D), Fe⁺ (a⁴F), and Co⁺, respectively. (Cross section information for Ni⁺ + CH₄ has not been published.) The increase in total reactivity and the larger contribution of MSiH_x⁺ species is reasonable as the Si-H bonds of silane are weaker than the C-H bonds in methane.

Experimental and theoretical results indicate that there is a barrier in the exit channel for dehydrogenation of methane by Fe⁺ and Co⁺.^{12,54,56-58} We believe that such barriers are unlikely in the silane systems for several reasons. First, dehydrogenation of silane is 2.3 eV more favorable than dehydrogenation of methane. Second, previous work in our laboratory and others has demonstrated that hydrogen atom migrations are facile on silicon centers.^{50,59,60} The increased hydrogen mobility at silicon centers would allow more efficient production of MSiH₂⁺ in the silane systems as compared to production of MCH₂⁺ in the methane systems. This is consistent with the large contribution to the total reactivity of MSiH₂⁺ vs MCH₂⁺. Third, as mentioned above, the ¹A₁ ground state of SiH₂ may form a donor-acceptor type σ-bond by donating nonbonding electrons into an empty 4s orbital on the metal ion. The ³B₁ ground state of CH₂ is not able to accomplish such an interaction. Fourth, as will be discussed below, reactions of silane with Fe⁺, Co⁺, and Ni⁺ likely occur through a statistically behaved intermediate, whereas reactions with methane proceed through more direct pathways which favor production of MH⁺ and MCH₃⁺ over MCH₂⁺.

Reaction Mechanism. The competition between the various

(53) Armentrout, P. B.; Beauchamp, J. L. *J. Am. Chem. Soc.* **1981**, *103*, 784.

(54) Haynes, C. L.; Armentrout, P. B. Work in progress.

(55) Halle, L. F.; Armentrout, P. B.; Beauchamp, J. L. *Organometallics* **1982**, *1*, 963.

(56) Jacobson, D. B.; Freiser, B. S. *J. Am. Chem. Soc.* **1985**, *107*, 4373.

(57) Chen, Y.-M.; Armentrout, P. B. Work in progress.

(58) Musaev, D. G.; Morokuma, K.; Koga, N.; Nguyen, K. A.; Gordon, M. S.; Cundari, T. R. *J. Phys. Chem.* **1993**, *97*, 11435.

(59) Kickel, B. L.; Fisher, E. R.; Armentrout, P. B. *J. Phys. Chem.* **1992**, *96*, 2603.

(60) Mandich, M. L.; Reents, W. D., Jr.; Jarrold, M. F. *J. Chem. Phys.* **1988**, *88*, 1703. Mandich, M. L.; Reents, W. D., Jr.; Kolenbrander, K. D. *J. Chem. Phys.* **1990**, *92*, 437.

(47) Armentrout, P. B.; Clemmer, D. E., In *Energetics of Organometallic Species*; Simoes, J. A. M., Ed.; Kluwer: Dordrecht, Netherlands, 1992; pp 321-356.

(48) Armentrout, P. B. *ACS Symp. Ser.* **1990**, *428*, 18.

(49) Dalleska, N. F.; Honma, K.; Sunderlin, L. S.; Armentrout, P. B. *J. Am. Chem. Soc.* **1994**, *116*, 3519.

(50) Boo, B. H.; Armentrout, P. B. *J. Am. Chem. Soc.* **1987**, *109*, 3549.

(51) Trinquier, G. *J. Am. Chem. Soc.* **1990**, *112*, 2130, and references therein.

(52) Grev, R. S.; Schaefer, H. F. *J. Chem. Phys.* **1992**, *97*, 7990.

product channels and the state-specific chemistry observed here is easily understood in terms of intermediate **I**, $\text{H}-\text{M}^+-\text{SiH}_3$, formed by inserting M^+ into a $\text{Si}-\text{H}$ bond of silane. The analogous intermediate has been suggested for the reaction of Si^+ with SiH_4 and for M^+ with CH_4 .⁶¹⁻⁶⁴ Because the $\text{H}-\text{SiH}_3$ bond is weaker than $\text{H}-\text{CH}_3$, the M^+ insertion should be more facile in the silane than carbon systems. In addition, Ferhati and Ohanessian find **I** to be the key intermediate in their calculations of the $\text{Y}^+ + \text{SiH}_4$ reaction surfaces.¹⁰ Although the structure of **I** is a reasonable choice for the reaction intermediate, consideration should also be given to the possibility that bridged isomers, e.g., $\text{M}^+(\text{H})\text{SiH}_3$ or $\text{M}^+(\text{H}_2)\text{SiH}_2$, are involved instead. Such intermediates have also been postulated for the $\text{Si}^+ + \text{SiH}_4$ system,⁶³ but theoretical calculations of Raghavachari do not find these to be important.⁶⁴ Neither are they found to be important in the $\text{Y}^+ + \text{SiH}_4$ calculations.¹⁰ The remainder of this discussion proceeds on the assumption that the primary intermediate has structure **I**, although the present results cannot be used to determine which of the MH_2Si^+ structures may be most important. This assumption is not meant to imply that different structures of the intermediates and products cannot be formed as the energy available to the system is increased. (It is useful to note that the qualitative ideas concerning the reaction mechanisms discussed below find parallels in the $\text{Si}^+ + \text{SiH}_4$ system,⁶²⁻⁶⁴ although the quantitative aspects of these results are not directly applicable to the MSiH_4^+ systems because the two heavy atoms in this complex are different while they are identical in the Si_2H_4^+ system.)

There are two possible pathways for the dehydrogenation of **I** to form MSiH_2^+ . The first possibility involves hydrogen atom migration after insertion to form intermediate **II**, $\text{H}_2\text{M}^+-\text{SiH}_2$. Formation of **II** is more reasonable in the silane systems than in the methane systems because of the decreased strength of the $\text{Si}-\text{H}$ bonds, greater mobility of hydrogen atoms on silicon centers,^{50,59,60} and the possibility that $\text{SiH}_2(^1\text{A}_1)$ can form a simple donor bond with M^+ . Subsequent 1,1-reductive elimination of molecular hydrogen from **II** produces MSiH_2^+ . The second possibility is a four-centered elimination of molecular hydrogen from **I**, which should be considered for two reasons. First, if **II** were being formed, we might have observed formation of MH_2^+ , which was not the case, although this product is observed for the group 3 metal ions⁶⁵ where it is thermodynamically more favorable.^{37,66} Second, theoretical calculations⁶⁷ have demonstrated that a four-centered elimination can occur with little or no barrier if the metal-ligand bonds are covalent and have substantial d character, as would be the case in **I**. Ferhati and Ohanessian considered both pathways for dehydrogenation of silane by Y^+ and concluded that the four-centered elimination was the lowest energy pathway and formed the Y^+-SiH_2 structure.¹⁰

The competition between formation of $\text{MSiH}_2^+ + \text{H}_2$ and $\text{MH}^+ + \text{SiH}_3$ or $\text{MH} + \text{SiH}_3^+$ in reactions 7, 4, and 9, respectively, may be explained in terms of a common intermediate like **I**. At the lowest energies the dominant product is

(61) Armentrout, P. B. In *Gas Phase Inorganic Chemistry*; Russell, D. H., Ed.; Plenum: New York, 1989; pp 1-41.

(62) The qualitative aspects of the reaction mechanism for $\text{Si}^+ + \text{SiH}_4$ were first examined by Boo and Armentrout.⁶³ Subsequent calculations of Raghavachari⁶⁴ elucidated the most important pathways and intermediates.

(63) Boo, B. H.; Armentrout, P. B. *J. Am. Chem. Soc.* **1987**, *109*, 3549.

(64) Raghavachari, K. *J. Chem. Phys.* **1988**, *88*, 1688.

(65) Kickel, B. L.; Armentrout, P. B. *J. Am. Chem. Soc.*, submitted for publication.

(66) Sunderlin, L. S.; Armentrout, P. B. *J. Am. Chem. Soc.* **1989**, *111*, 3845.

(67) Steigerwald, M. L.; Goddard, W. A. *J. Am. Chem. Soc.* **1984**, *106*, 308.

MSiH_2^+ , indicating that elimination of H_2 is thermodynamically favored. As the available energy is increased, decomposition of **I** through reaction 4 or 9 is kinetically favored despite being more endothermic, because reactions 4 and 9 proceed through looser transition states than reaction 7. As discussed previously, conservation of angular momentum also favors production of $\text{MH}^+ + \text{SiH}_3$ or $\text{MH} + \text{SiH}_3^+$ over $\text{MSiH}_2^+ + \text{H}_2$.⁶⁸ It is also possible that formation of $\text{MH}^+ + \text{SiH}_3$ for $\text{M} = \text{Fe}$ may occur via more direct pathways than simple decomposition of **I**, as suggested by the observation that the maximum cross section of FeH^+ is greater than the maximum in the FeSiH_2^+ cross section. However, the maximum cross sections for CoH^+ , NiH^+ , and SiH_3^+ are smaller than those of CoSiH_2^+ and NiSiH_2^+ , indicating that CoH^+ , NiH^+ , and SiH_3^+ may be formed exclusively through decomposition of **I**. Another higher energy decomposition pathway available to intermediate **I** is dissociation by $\text{M}-\text{H}$ bond cleavage to form $\text{MSiH}_3^+ + \text{H}$. Further decomposition of MSiH_3^+ and MSiH_2^+ by dehydrogenation yields MSiH^+ and MSi^+ , respectively.

Branching Ratios. Branching ratios for competing reactions such as reactions 4 and 8 have been found to be a sensitive indicator of reaction mechanism. Previously we have discussed the arguments involved for the reaction of V^+ with methane.⁶⁸ The same arguments may be applied to the reactions of Fe^+ , Co^+ , and Ni^+ with silane. Simple arguments involving conservation of energy and angular momentum in direct reactions lead to a general expression for the branching ratio between reactions 4 and 8 (indicated by the subscripts),

$$\sigma_4(\text{MH}^+)/\sigma_8(\text{MSiH}_3^+) = [(\alpha E)^{1/2}/\mu]_4/[(\alpha E)^{1/2}/\mu]_8 \quad (14)$$

where α is the polarizability of the neutral product [$\alpha_4 = \alpha(\text{SiH}_3)$, $\alpha_8 = \alpha(\text{H}) = 0.67 \text{ \AA}^3$],⁶⁹ μ is the reduced mass of the products, and E is the relative translational energy of the products. As discussed previously,⁶⁸ this formula reduces to $\sigma(\text{MH}^+)/\sigma(\text{MCH}_3^+) = 20[E(\text{MH}^+)/E(\text{MCH}_3^+)]^{1/2}$ for the methane systems. For the silane systems, we find $\sigma(\text{MH}^+)/\sigma(\text{MSiH}_3^+) = 51[E(\text{MH}^+)/E(\text{MSiH}_3^+)]^{1/2}$ where averaged reduced masses for $\text{M} = \text{Fe}$, Co , and Ni are used and $\alpha(\text{SiH}_3) = 4.23 \text{ \AA}^3$, as calculated by using the methods outlined by Miller and Savchik.⁷⁰ Because the endothermicities of reactions 4 and 8 are comparable for each metal system (Table 3), the relative translational energies of these two product channels should be similar, such that the $E(\text{MH}^+)/E(\text{MSiH}_3^+)$ term should be near unity for all reactant kinetic energies. Thus, formula 14 predicts that direct reactions will have branching ratios between reactions 4 and 8 of about 50 or more. We anticipate that branching ratios considerably smaller than this correspond to more statistically behaved reactions on the basis of our previous work in the methane systems.⁶⁸

Experimentally, the branching ratios (taken at the peak of the MSiH_3^+ cross section) for Fe^+ are observed to be dependent on the electronic state. The ratio is ~ 3 for the $a^6\text{D}$ state and ~ 13 for the $a^4\text{F}$ state. The branching ratios for ground state Co^+ and Ni^+ are ~ 14 and ~ 3 , respectively. Therefore, we conclude that Fe^+ , Co^+ , and Ni^+ react with silane through a statistically behaved intermediate. It is also important to check whether this conclusion is altered by the competition between formation of $\text{MH}^+ + \text{SiH}_3$ and $\text{SiH}_3^+ + \text{MH}$, reactions 4 and 9, respectively, and decomposition of MSiH_3^+ by dehydrogenation to form MSiH^+ . This competition means that the branching ratio is more appropriately determined as $\sigma_4/\sigma_8 = [\sigma(\text{MH}^+) + \sigma(\text{SiH}_3^+)]/[\sigma(\text{MSiH}_3^+) + \sigma(\text{MSiH}^+)]$. These ratios

(68) Aristov, N.; Armentrout, P. B. *J. Phys. Chem.* **1987**, *91*, 6178.

(69) Miller, T. M.; Bederson, B. *Adv. At. Mol. Phys.* **1977**, *13*, 1.

(70) Miller, K. J.; Savchik, J. A. *J. Am. Chem. Soc.* **1979**, *101*, 7206.

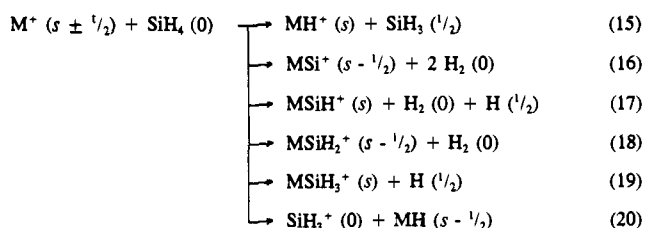
are 7, 1, 11, and 10 for Fe⁺ (a⁴D), Fe⁺ (a⁶D), Co⁺ (a³F), and Ni⁺ (a²D), respectively. These ratios are still consistent with a statistically behaved intermediate, but show more consistent behavior between Fe⁺ (a⁴F), Co⁺, and Ni⁺.

In contrast to these results, the reactions of methane with Fe⁺ and Co⁺ yield branching ratios consistent with more direct pathways.^{12,54} This helps explain the differences between the reactivity of these ions with methane and silane. Direct pathways favor the production of MH⁺ and MCH₃⁺, which are the only products observed for Fe⁺ (a⁶D and a⁴F). In the silane systems, the longer lived statistical intermediate helps permit the more complex dehydrogenation reaction to compete effectively.

Molecular Orbital and Spin Considerations. In order to understand the state-specific results obtained here, we use simple molecular orbital and spin conservation arguments. Oxidative addition of a Si-H bond to a metal center is achieved by donation of the σ -bonding electrons into an empty 4s orbital of the metal and back-donation of metal 3d π electrons into the σ^* antibonding orbital. This results in an increase of electron density between the metal and the molecular fragment and a lengthening of the Si-H bond. Furthermore, this simple picture would predict that metals in states that have an occupied 4s orbital will have repulsive interactions as they approach the Si-H bonding σ electrons. This explains why ground state Fe⁺ (a⁶D, 4s3d⁶) is much less reactive than excited state Fe⁺ (a⁴F, 3d⁷) and the ground states of Co⁺ (a³F, 3d⁸) and Ni⁺ (a²D, 3d⁹).

An additional factor that should be considered in the reactivity of metal ions is the spin state of the reactants and products. The molecular orbital arguments make no distinction between high- and low-spin metal reactant state reactivity. On the basis of the present excited state results for Fe⁺ and previous results for Ti⁺, V⁺, and Cr⁺,⁵ the electronic energy of the metal ion is able to efficiently couple into the reaction coordinate; however, the effect of the electronic energy differs for various product channels. We can use spin conservation arguments to better understand this effect. Reactions 15–20 show the spin states of the individual species for the observed reactions, and the number in parentheses is the spin quantum number of that particular species. The value of s is chosen to represent the ground state of the MH⁺ product; therefore, $s = 2, 3/2,$ and 1 for FeH⁺, CoH⁺, and NiH⁺, respectively, indicating that these species have quintet, quartet, and triplet spins.⁷¹ The indicated spin states for SiH₄, H₂, H, SiH₃⁺, and MH are known.^{44,72,73} Those for MSiH₂⁺ have been calculated.⁸ We assume that MSiH₃⁺ has a single M-Si covalent bond and therefore has the same spin state as MH⁺. The spins of MSiH⁺ and MSi⁺ are assumed to be the same as their precursors, MSiH₃⁺ and MSiH₂⁺, respectively.

Reactions 16, 18, and 20 are spin-allowed for low-spin ($s - 1/2$) but not high-spin ($s + 1/2$) states of M⁺. This is consistent with the large enhancement observed for these



reactions by excited Fe⁺ (a⁴F). The observation that the high-spin ground state Fe⁺ (a⁶D) reacts to produce FeSiH₂⁺ + H₂ and SiH₃⁺ + FeH implies that there must be spin-orbit coupling between the high- and low-spin surfaces. The relatively inefficient reactivity of the high-spin state compared with the low-spin excited state implies that this coupling is poor. For reaction 20, the enhancement in the production of SiH₃⁺ observed for low-spin Fe⁺ can also be explained by noting that the electronic configuration of the high-spin ground state, (a⁶D, 4s3d⁶), is not suitable for accepting H⁻ from SiH₄.

Reactions 15, 17, and 19 are spin-allowed from both ($s \pm 1/2$) spin states, which explains why the relative cross sections for FeSiH₃⁺ and FeSiH⁺ are larger for reaction of Fe⁺ (a⁶D) than for Fe⁺ (a⁴F). However, these cross sections and that for FeH⁺ show an absolute enhancement for excited state Fe⁺ (a⁴F) compared to Fe⁺ (a⁶D), Figure 5 and 6. As discussed above, all these products can be formed through the common intermediate I, which will have a low-spin ground state if both bonds to the metal are covalent. Formation of I therefore occurs diabatically from states having the correct spin and electronic configuration. The states that meet these requirements are the low-spin states of Fe⁺ (a⁴F, 3d⁷), Co⁺ (a³F, 3d⁸), and Ni⁺ (a²D, 3d⁹). This would explain the observed enhancement compared to Fe⁺ (a⁶D, 4s3d⁶).

Summary

In this study, we have examined the reactions of silane with Fe⁺, Co⁺, and Ni⁺. Threshold analyses of the cross sections allow the measurement of 0 K bond dissociation energies for M⁺-SiH_x ($x = 0-3$) and M-H. In agreement with theoretical predictions,^{8,9} the M⁺-SiH₂ bond energies are weaker than the M⁺-CH₂ bond energies. Trends in metal-silicon bond energies were discussed, although a definitive understanding of these trends is complicated because the most important structures for the MSiH_x⁺ species cannot be determined from the present results.

We have found that the reactions are more efficient for the low-spin a⁴F state of Fe⁺ than for the a⁶D ground state. This suggests the existence of a low-spin intermediate that we discussed in terms of a H-M⁺-SiH₃ structure, consistent with the calculations of Ferhati and Ohanessian,¹⁰ although bridged isomers M⁺(H)SiH₃ or M⁺(H₂)SiH₂ may also be involved. Although formation of this intermediate is spin-forbidden from the high-spin sextet ground state of Fe⁺, this state is observed to react to form low-spin products, indicating that spin-orbit coupling to the low-spin surfaces does occur. The relative efficiency of the ground and excited states suggests that this coupling is rather poor.

Acknowledgment. This work was supported by the National Science Foundation under Grant CHE-9221241.

JA941939L

(71) Ab initio calculations (Schilling, J. B.; Goddard, W. A.; Beauchamp, J. L. *J. Am. Chem. Soc.* **1986**, *108*, 582) predict the ground states of FeH⁺ (⁵ Δ), CoH⁺ (⁴ Φ), and NiH⁺ (³ Δ).

(72) Chase, M. W.; Davies, C. A.; Downey, J. R., Jr.; Frurip, D. J.; McDonald, R. A.; Syverud, A. N. *J. Phys. Chem. Ref. Data Suppl.* **1985**, *14*, No. 1 (JANAF Tables).

(73) Chong, D. P.; Langhoff, S. R.; Bauschlicher, C. W.; Walch, S. P.; Partridge, H. *J. Chem. Phys.* **1986**, *85*, 2850. The metal hydride ground states are FeH (⁴ Δ), CoH (⁴ Φ), and NiH (² Δ).